2-15-2019

Atoh1 $^{+}$ secretory progenitors possess renewal capacity independent of Lgr5 $^{+}$ cells during colonic regeneration

David Castillo-Azofeifa
University of California, San Francisco

Elena N. Fazio
Western University

Roy Nattiv
University of California, San Francisco

Hayley J. Good
Western University

Tomas Wald
University of California, San Francisco

See next page for additional authors

Article

TRANSPARENT PROCESS

THE EMBO JOURNAL

Atoh1$^+$ secretory progenitors possess renewal capacity independent of Lgr5$^+$ cells during colonic regeneration

David Castillo-Azofeifa[1,†], Elena N Fazio[2,†], Roy Nattiv[1,3,†], Hayley J Good[2], Tomas Wald[1], Michael A Pest[4], Frederic J de Sauvage[5], Ophir D Klein[1,3,6,*] & Samuel Asfaha[2,**]

Abstract

During homeostasis, the colonic epithelium is replenished every 3–5 days by rapidly cycling *Lgr5*$^+$ stem cells. However, various insults can lead to depletion of *Lgr5*$^+$ stem cells, and colonic epithelium can be regenerated from *Lgr5*-negative cells. While studies in the small intestine have addressed the lineage identity of the *Lgr5*-negative regenerative cell population, in the colon this question has remained unanswered. Here, we set out to identify which cell(s) contribute to colonic regeneration by performing genetic fate-mapping studies of progenitor populations in mice. First, using *keratin*-19 (*Krt19*) to mark a heterogeneous population of cells, we found that *Lgr5*-negative cells can regenerate colonic crypts and give rise to *Lgr5*$^+$ stem cells. *Notch1*$^+$ absorptive progenitor cells did not contribute to epithelial repair after injury, whereas *Atoh1*$^+$ secretory progenitors did contribute to this process. Additionally, while colonic *Atoh1*$^+$ cells contributed minimally to other lineages during homeostasis, they displayed plasticity and contributed to epithelial repair during injury, independent of *Lgr5*$^+$ cells. Our findings suggest that promotion of secretory progenitor plasticity could enable gut healing in colitis.

Keywords Atoh1; colitis; Krt19; Notch1; stem cells
Subject Categories Development & Differentiation; Molecular Biology of Disease; Stem Cells
DOI 10.15252/embj.201899984 | Received 5 June 2018 | Revised 29 November 2018 | Accepted 30 November 2018 | Published online 11 January 2019
The EMBO Journal (2019) 38: e99984

Introduction

The colonic epithelium turns over every 5–7 days, driven by dividing stem cells located at the crypt base. Genetic lineage tracing studies in mice have demonstrated that leucine-rich repeat-containing G-protein-coupled receptor (*Lgr5*)-expressing crypt-based columnar (CBC) cells are the main cells that replenish both the small intestinal and colonic epithelium in normal homeostasis (Barker & Clevers, 2010). Additionally, other genes, such as *mTert*, *Lrig1*, or *Krt19*, have been reported to mark stem/progenitor cells that contribute to epithelial turnover in the colon (Montgomery *et al*, 2011; Powell *et al*, 2012; Asfaha *et al*, 2015). However, the inability to simultaneously use more than one Cre-based mouse lineage tracing model has led to challenges in distinguishing among the role of different progenitor or stem cell pools (Barker *et al*, 2007; Sangiorgi & Capecchi, 2008; Buczacki *et al*, 2013; Barriga *et al*, 2017).

We have previously demonstrated that when *Lgr5*$^+$ cells are ablated, cells marked by genes including *Bmi1* or *Krt19* can regenerate *Lgr5*$^+$ cells and their lineages in the small intestine or colon, respectively (Tian *et al*, 2011; Asfaha *et al*, 2015). In the context of injury, secretory (*Dll1* or *Prox1*) and absorptive (*Alpi*) cell lineages, as well as *Lgr5*-expressing Paneth cells, have been proposed to renew all the cells along the crypt–villus axis in the small intestine (van Es *et al*, 2012; Buczacki *et al*, 2013; Metcalfe *et al*, 2014; Tetteh *et al*, 2016; Yan *et al*, 2017). These data point to cellular plasticity in the intestinal epithelium, and, in particular, to the ability of more differentiated cells to revert to a stem cell fate within the crypt (Fre *et al*, 2011; Furuyama *et al*, 2011; Montgomery *et al*, 2011; Takeda *et al*, 2011; Powell *et al*, 2012). Notably, we and others have also reported that *Lgr5*$^+$ stem cells are highly sensitive to epithelial injury induced by radiation or colitis (Yan *et al*, 2012; Asfaha *et al*, 2015; Ishibashi *et al*, 2018), suggesting that an *Lgr5*-negative cell population is responsible, at least in part, for colonic regeneration. More recently, work by two groups suggested that secretory cells marked by the transcription factor *Atoh1* contribute to colonic epithelial repair (Ishibashi *et al*, 2018 and Tomic *et al*,

1 Department of Orofacial Sciences and Program in Craniofacial Biology, University of California, San Francisco, San Francisco, CA, USA
2 Department of Medicine, University of Western Ontario, London, ON, Canada
3 Department of Pediatrics, University of California, San Francisco, San Francisco, CA, USA
4 Department of Physiology & Pharmacology, University of Western Ontario, London, ON, Canada
5 Department of Molecular Oncology, Genentech, South San Francisco, CA, USA
6 Institute for Human Genetics, University of California, San Francisco, San Francisco, CA, USA
*Corresponding author. Tel: +1 415 476 4719; E-mail: ophir.klein@ucsf.edu
**Corresponding author. Tel: +1 519 685 8500; 53293; E-mail: sasfaha2@uwo.ca
†These authors contributed equally to this work

2018). However, neither study directly addressed whether *Atoh1*$^+$ cells are dependent on *Lgr5*$^+$ stem cells for this epithelial repair. It also remains unknown whether *Atoh1*$^+$ progenitors are required for colonic epithelial repair and whether the cellular plasticity of these cells extends to epithelial cells of the absorptive cell lineage.

Identifying *Lgr5*-negative progenitors in the colon, as opposed to small intestine, has proven challenging due to the paucity of distinct stem cell markers. Here, we confirm that *Lgr5*$^+$ stem cells are dispensable for colonic regeneration in colitis and determine the contribution of various *Lgr5*-negative colonic progenitors to epithelial regeneration following colonic injury. Using genetic fate-mapping models for labeling of *keratin*-19 (*Krt19*) expressing cells or absorptive (*Notch1*) and secretory (*Atoh1*) progenitors, we carried out lineage tracing and cell-specific ablation studies in the context of DSS colitis to test the functional contribution of each progenitor or stem cell population to epithelial regeneration.

Results

Lrg5$^+$ stem cells are sensitive to colonic injury and dispensable for epithelial regeneration post-colitis

To determine whether *Lgr5*$^+$ cells contribute to colonic epithelial regeneration post-colitis, we performed genetic fate-mapping studies using *Lgr5*$^{GFP\text{-}IRES\text{-}CreERT2}$;*ROSA26*^{tdTomato} (Barker *et al*, 2007; Madisen *et al*, 2010) mice that were administered 5 days of 2.5–3% dextran sodium sulfate (DSS) in the drinking water (Fig 1A). Compared to control mice that were administered regular drinking water, DSS-treated mice showed complete crypt destruction and epithelial damage with a marked infiltration of inflammatory cells within the lamina propria at days 5–10, and regeneration of crypts occurred by days 10–12 (Fig 1C). Consistent with previous reports (Okayasu *et al*, 1990; Cooper *et al*, 1993; Laroui *et al*, 2012), we found that the distal colon was the most severely injured colonic segment after DSS. Therefore, we focused our analysis on the distal colon. After 5 days of DSS colitis, we observed complete loss of *Lgr5* mRNA expression predominantly in the distal colon, as assessed by RNAscope single molecule *in situ* hybridization (Fig 1B). Consistent with our RNAscope data, we observed that *Lgr5*-GFP$^+$ cells were absent from the crypt base immediately following and up until 5 days post-DSS (day 10; Fig 1D and E). Control *Lgr5*$^{GFP\text{-}IRES\text{-}CreERT2}$;*ROSA26*^{tdTomato} mice showed fully labeled tdTomato$^+$ lineage-traced crypts as early as 4 days after initial tamoxifen induction of Cre recombinase (day 8; Fig 1D and E), whereas in DSS-treated mice, tdTomato$^+$ lineage-traced crypts were not detectable within the colonic epithelium at any of the time points examined after treatment was begun (Fig 1D and E), consistent with the absence of *Lgr5*$^+$ cells (Davidson *et al*, 2012). In line with recent work on the regeneration of intestinal *Lgr5*$^+$ cells following injury or ablation (Tian *et al*, 2011; Metcalfe *et al*, 2014; Asfaha *et al*, 2015) by 7 days post-DSS (day 12), we observed a return of *Lgr5*-GFP$^+$ cells at the crypt base (Fig 1D). Indeed, the loss of *Lgr5*$^+$ cells post-DSS colitis was consistent with our RT–PCR analysis of stem and progenitor cell markers, which revealed that *Lgr5* mRNA expression was the most reduced transcript post-DSS, with nearly a 15-fold reduction compared to control mice (Fig 1F).

Given that *Lgr5*$^+$ stem cells were sensitive to colitis injury, we tested whether these cells were functionally required for colonic epithelial regeneration. We administered diphtheria toxin (DT) to ablate *Lgr5*$^+$ cells in *Lgr5*$^{DTR\text{-}GFP}$ transgenic mice during and for 5 days following DSS, and we examined the effects on body weight, colonic histology, and overall survival (Fig 1G–K). We observed no difference in body weight or overall survival up to 12 days following initiation of DSS after ablating *Lgr5*$^+$ cells (Fig 1H and I). Confirming previously reported findings, we did not detect any difference in the degree of colonic epithelial injury or inflammation between saline- and DT-treated groups as assessed by histology (Fig 1J and K; Metcalfe *et al*, 2014). To conclusively assess the absence of *Lgr5*$^+$ stem cells post-DT treatment, we carried out RNAscope to examine *Lgr5* mRNA expression along the anteroposterior colonic epithelium. In contrast to DSS injury, DT treatment resulted in complete loss of *Lgr5* expression throughout the colon (Fig 1L).

Lgr5-negative/*Krt19*$^+$ cells contribute to colonic epithelial regeneration in colitis

Since *Lgr5*$^+$ cells were dispensable for colonic epithelial regeneration in colitis, we next asked which *Lgr5*-negative cell population was responsible for colonic epithelial regeneration post-colitis. We

Figure 1. *Lgr5*$^+$ stem cells are sensitive to colonic injury and dispensable for epithelial regeneration in colitis.

A Illustration of experimental protocol outlining DSS-induced colitis in *Lgr5*$^{GFP\text{-}CreERT2}$;*ROSA26*^{tdTomato} mice.
B RNAscope analysis of *Lgr5* mRNA in DSS colitis demonstrating loss of *Lgr5* transcript (N = 3 per condition).
C Hematoxylin and eosin staining of the colonic epithelium following DSS-induced damage. Crypts are dramatically injured by d5. At d8 through d12, regenerating crypts are observed.
D, E Compared to untreated controls, DSS treatment ablates *Lgr5*-GFP$^+$ stem cells and results in functional loss of tdTomato$^+$ lineage tracing as early as d5. *Lgr5*-GFP$^+$ stem cells reappear by d12 (N = 3–4 per condition).
F Effects of DSS colitis injury on RNA expression levels of stem (*Lgr5* and *Krt19*) and progenitor (*Atoh1* and *Notch1*) cell markers. *Lgr5* mRNA expression is significantly decreased after exposure to DSS (N = 6–7 per condition).
G DSS and DT treatment of *Lgr5*$^{DTR\text{-}GFP}$ mice.
H, I Mice body weight (H) and survival (I) are comparable between three treatments: DSS + DT (N = 12), only DSS (N = 8), or only DT (N = 3).
J Hematoxylin and eosin staining of the colonic epithelium shows no morphological difference between DSS alone and DSS + DT-treated mice.
K The extent of epithelial damage is similar in mice treated with DSS alone versus DSS + DT (to ablate *Lgr5*$^+$ stem cells; N = 3 DSS; N = 6 DSS + DT).
L RNAscope for *Lgr5* in *Lgr5*$^{DTR\text{-}GFP}$ mice showing loss of *Lgr5* transcripts after DT treatment (N = 3–4 per condition).

Data information: Nuclei are counterstained with Dapi (blue); white dashed lines indicate basement membrane. Scale bars (B, C, D, L) = 50 μm; scale bar (J) = 500 μm. Data are represented as mean ± SD (E) and mean ± SEM (F–K) analyzed using Student's t-test. *$P \leq 0.05$, **$P \leq 0.01$.

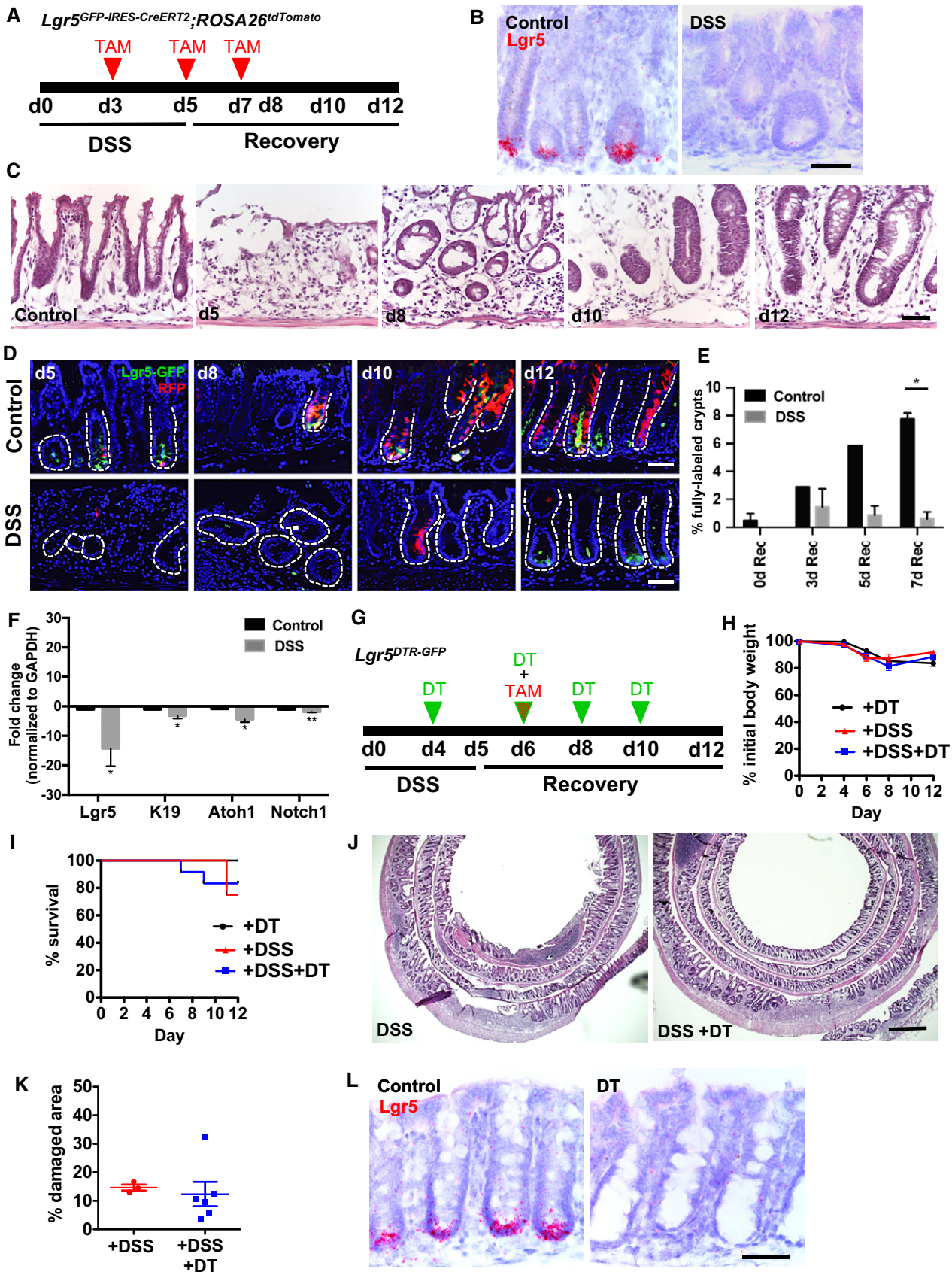
A
Lgr5GFP-IRES-CreERT2;ROSA26tdTomato
TAM
TAM
TAM
d0
d3
d5
d7 d8
d10
d12
DSS
Recovery
B
Control
Lgr5
DSS
C
Control
d5
d8
d10
d12
D
Control
DSS
d5
Lgr5-GFP
RFP
d8
d10
d12
E
% fully-labeled crypts
Control
DSS
0d Rec
3d Rec
5d Rec
7d Rec
F
Fold change (normalized to GAPDH)
Control
DSS
Lgr5
K19
Atoh1
Notch1
G
Lgr5DTR-GFP
DT
DT + TAM
DT
DT
d0
d4
d5
d6
d8
d10
d12
DSS
Recovery
H
% initial body weight
+DT
+DSS
+DSS+DT
Day
I
% survival
+DT
+DSS
+DSS+DT
Day
J
DSS
DSS +DT
K
% damaged area
+DSS
+DSS +DT
L
Control
Lgr5
DT

Figure 1.

first examined the role of *Krt19*$^+$ cells, as we previously showed that this marker labels intestinal and colonic crypt cells, but excludes rapidly cycling *Lgr5*$^+$ stem cells (Asfaha *et al*, 2015; Figs 2B and EV1A–C). To examine the role of *Krt19*$^+$ cells in colonic regeneration, we crossed *Krt19*$^{BAC\text{-}CreERT2}$ mice (Asfaha *et al*, 2015) to *ROSA26*^{tdTomato} reporter mice and performed genetic lineage tracing studies in the setting of DSS colitis (Fig 2A). Consistent with our previously reported findings, during homeostasis the *Krt19*$^+$ cells showed the capacity to lineage trace entire colonic crypts, including *Lgr5*-GFP$^+$ cells, at 8–10 days following tamoxifen induction (Fig 2B). *Krt19*$^+$ cells continued to lineage trace entire colonic crypts throughout the regenerative period following DSS colitis as well as give rise to new *Lgr5*-GFP$^+$ cells by 12 days after initiation of DSS (Fig 2B and C). Quantification of contiguously labeled *Krt19*$^+$ crypts, indicative of crypt fission as previously described (Okayasu *et al*, 1990; Park *et al*, 1995; Hirata *et al*, 2013), revealed an increase in lineage-traced crypts, consistent with regeneration over the 12-day time interval examined (Fig 2C).

Given that *Krt19*$^+$ cells renewed the epithelium post-DSS colitis, we next examined the effects of conditional *Krt19*$^+$ cell ablation in the setting of DSS-induced colitis. We crossed *Krt19*$^{BAC\text{-}CreERT2}$;*ROSA26*^{tdTomato} mice and *ROSA26*^{DTR} mice in order to allow us to selectively ablate DTR-expressing cells following DT administration. We administered tamoxifen to induce Cre-mediated expression of DTR, followed by DT administration (Fig 2D), which ablated nearly all *Krt19*-tdTomato$^+$ cells in *Krt19*$^{BAC\text{-}CreERT2}$;*ROSA26*$^{tdTomato/DTR}$ mice (Fig 2E and F). Surprisingly, DT ablation of *Krt19*$^+$ cells did not alter the survival or colonic histology of mice with colitis (Fig 2G and H), suggesting that *Krt19*$^+$ cells may also be dispensable for renewal. Concurrent DSS colitis and *Krt19*$^+$ cells ablation did not affect body weight and overall animal survival (Fig 2G); however, it did cause a significant increase in colonic histologic damage when compared to saline-treated controls (Fig 2H and I). Taken together, these data indicate that *Krt19*-expressing cells contribute to epithelial regeneration within the colon.

We previously showed that *Krt19* labels a heterogeneous population of cells within the crypt (Asfaha *et al*, 2015), including both absorptive and secretory cells. Thus, we further assessed whether *Krt19* is expressed in all secretory cells or only a subset of cells within the colon. We examined colonic tissue sections from *Krt19*$^{BAC\text{-}CreERT2}$;*ROSA26*^{tdTomato} mice 24 h post-tamoxifen and looked for co-localization of various secretory cell markers with TdTomato$^+$ cells. By immunofluorescence staining, we detected overlap of TdTomato$^+$ with *ChgA*, *Dclk1*, and Muc2 expression, indicating that *Krt19* indeed marks a variety of secretory cells including enteroendocrine, tuft, and goblet cells, respectively (Fig EV2A and B).

Colonic *Notch1*$^+$ absorptive progenitors do not contribute to epithelial repair in homeostasis or injury

We next sought to precisely define the *Lgr5*-negative/*Krt19*$^+$ population that contributes to epithelial regeneration in colitis and assessed whether an absorptive or progenitor cell plays a major role in epithelial repair. We assayed the contribution of absorptive progenitors, defined by expression of *Notch1* (van Es *et al*, 2005; Riccio *et al*, 2008; Pellegrinet *et al*, 2011), in colonic regeneration, by using *Notch1*^{CreERT2} mice (Fre *et al*, 2011) crossed to *ROSA26*^{tdTomato} mice. In control mice, at day 5 (2 days following the initial tamoxifen dose), *Notch1*$^+$ cells were found dispersed throughout the colonic crypt, consistent with the labeling of absorptive progenitors and their progeny (Fig 3B). In rare instances (~1–2% of crypts), we observed entire crypts lineage traced by day 12, consistent with previous reports of *Notch1* expression within *Lgr5*$^+$ stem cells (Fig 3B; Itzkovitz *et al*, 2012), and we detected rare *Notch1*-expressing *tdTomato*$^+$ cells that co-localized with *Lgr5*-GFP$^+$ expression (Fig 3B). To further assess whether *Notch1*$^+$ absorptive progenitors and/or their progeny contribute to colonic regeneration following colitis injury, we administered DSS to *Notch1*^{CreERT2};*ROSA26*^{tdTomato} mice and examined tdTomato$^+$ lineage tracing (Fig 3B). In the setting of DSS colitis, *Notch1*$^+$ cells appeared sensitive to injury, with very rare tdTomato$^+$ cells being detectable by day 10 (5 days post-DSS) and no fully lineage-traced colonic crypts being detected at days 10–12 (Fig 3B and C). Next, we carried out *Notch1*$^+$ lineage tracing studies in the presence or absence of *Lgr5*$^+$ cell ablation with DT in *Notch1*^{CreERT2};*ROSA26*^{tdTomato} crossed to *Lgr5*$^{DTR\text{-}GFP}$ mice (Fig 3D). Indeed, *Notch1*$^+$ cell lineage tracing was no longer detectable upon DT ablation of *Lgr5*$^+$ cells (Fig 3E and F), suggesting that some *Notch1*-expressing cells also express *Lgr5*. Taken together, these findings indicate that *Notch1*$^+$ absorptive cells do not play a major role in colonic epithelial regeneration following DSS-induced colitis.

Atoh1$^+$ secretory progenitors display plasticity during both homeostasis and injury in colonic regeneration

Next, to determine the role of secretory progenitors and their progeny in colonic epithelial homeostasis and injury, we carried out genetic lineage tracing studies using *Atoh1*^{CreERT2} mice (Fujiyama *et al*, 2009) crossed to *ROSA26*^{tdTomato} mice. We examined tdTomato$^+$ lineage tracing in *Atoh1*^{CreERT2};*ROSA26*^{tdTomato} mice

Figure 2. *Lgr5*-negative/*Krt19*$^+$ cells contribute to epithelial renewal during homeostasis and following colitis.

A Illustration of experimental protocol outlining DSS-induced colitis in *Krt19*$^{BAC\text{-}CreERT2}$;*ROSA26*^{tdTomato} mice.

B, C *Krt19*$^+$ cells lineage trace entire colonic crypts during both normal homeostasis and injury (N = 3–4 per condition).

D DSS and DT treatment of *Krt19*^{CreERT2};*ROSA26*$^{tdTomato/DTR}$ mice.

E, F DT ablation of *Krt19*$^+$ cells significantly reduced the number of lineage-labeled crypts ($N \geq 3$ per condition).

G Mice body weight and survival remain unchanged between DSS and DSS + DT-treated groups (N = 6 control; N = 7 DT).

H, I Hematoxylin and eosin staining of the colonic epithelium after DSS versus DSS + DT (H) and quantification of damaged epithelial area (I), showing more damage is seen in mice treated with both DSS + DT treatment (N = 6 control; N = 7 DT).

Data information: Nuclei are counterstained with Dapi (blue); white dashed lines outline the basement membrane. Scale bars (B) = 45 μm; scale bar (E) = 30 μm; scale bar (H) = 1 mm. Data are represented as mean ± SEM (C, F, G, I) using Student's t-test (F–I). *$P \leq 0.05$, **$P \leq 0.01$.

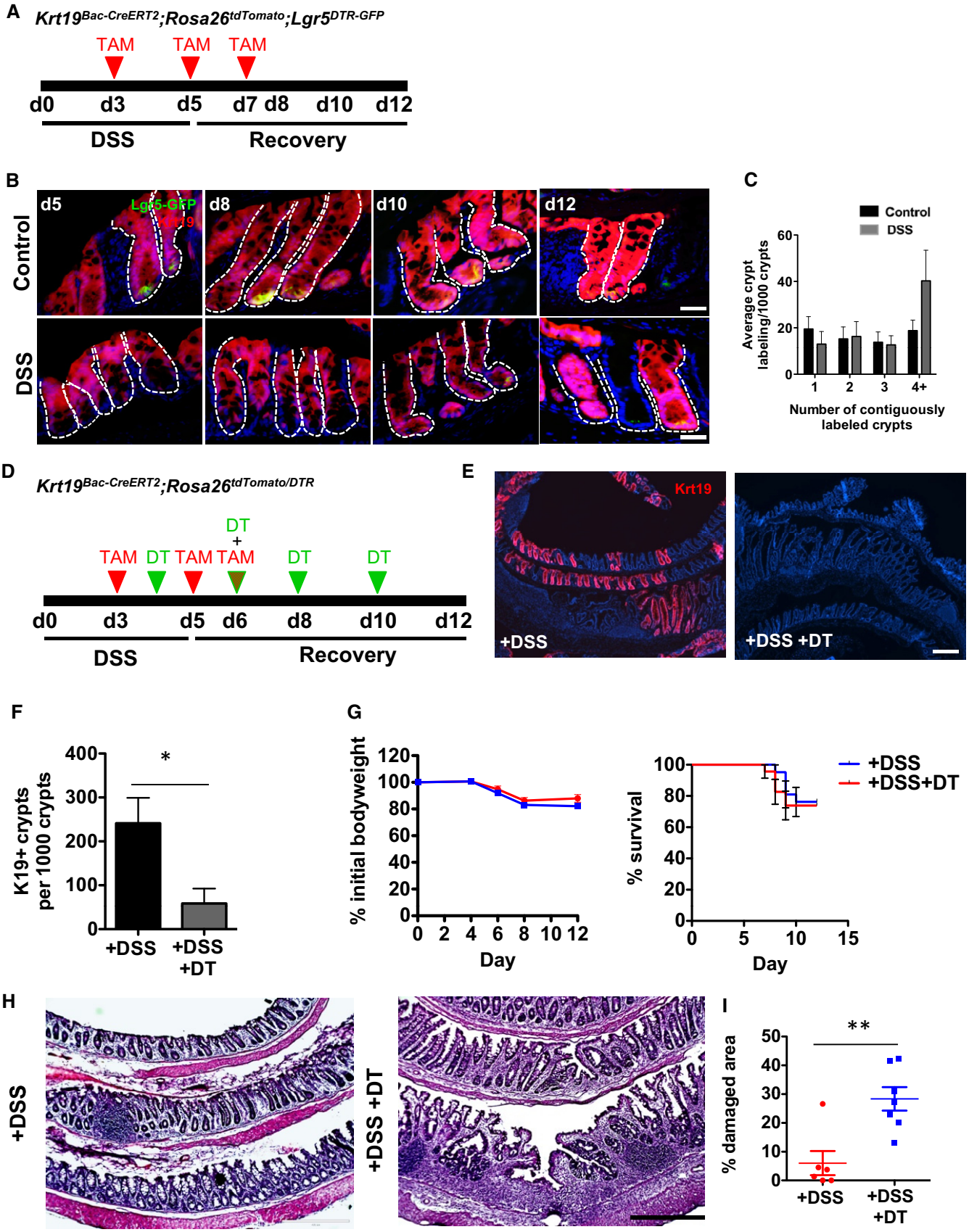

Figure 2.

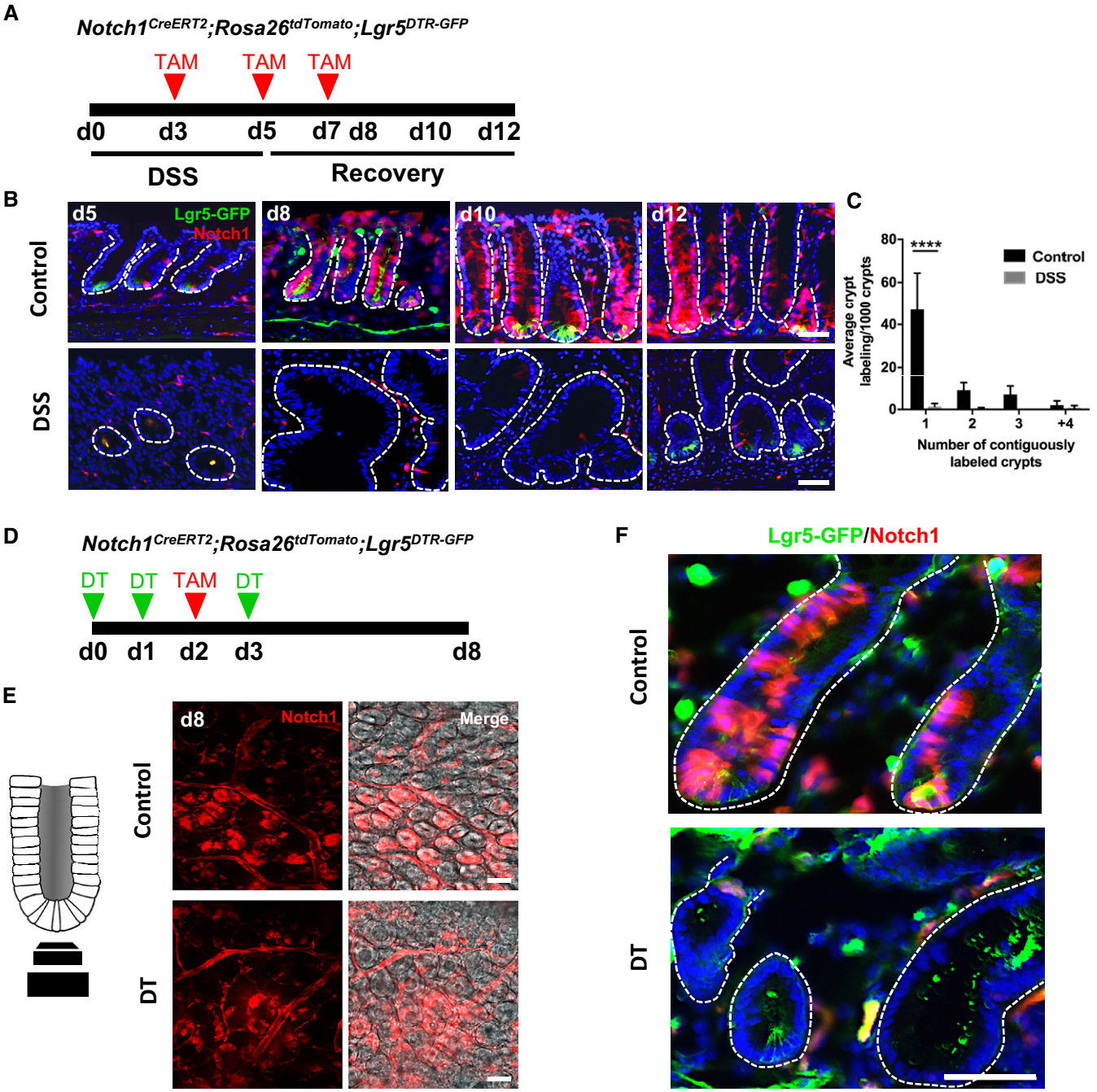

Figure 3. Colonic *Notch1*$^+$ absorptive progenitors aid in homeostatic renewal but do not show renewal capacity in injury.

A Illustration of experimental protocol outlining DSS-induced colitis in *Notch1*^{CreERT2};*ROSA26*^{tdTomato};*Lgr5*$^{DTR\text{-}GFP}$ mice.

B, C *Notch1*$^+$ progenitors are able to generate *Lgr5*$^+$ stem cells and contribute to epithelial renewal in homeostasis, however, do not contribute to regeneration after colitis (N = 4 per condition).

D Illustration of experimental protocol outlining DT ablation of *Lgr5*$^+$ cells in the context of *Notch1*$^+$ cell lineage tracing using *Notch1*^{CreERT2};*ROSA26*^{tdTomato};*Lgr5*$^{DTR\text{-}GFP}$ mice.

E, F Images of whole mount (E) and tissue sections (F) of *Notch1*^{CreERT2};*ROSA26*^{tdTomato};*Lgr5*$^{DTR\text{-}GFP}$ mice showing *Notch1* lineage-labeled crypts. No fully labeled crypts were found after *Lgr5*$^+$ stem cell ablation.

Data information: Nuclei are counterstained with Dapi (blue); white dashed lines indicate basement membrane. Scale bars = 50 μm. Data are represented as mean ± SD analyzed using two-way ANOVA with Sidak's multiple comparisons test. ****$P \leq 0.0001$.

administered DSS following the protocol illustrated in Figs 2A and 3A. In control mice, at day 5 (2 days after the initial tamoxifen dose), numerous *Atoh1*$^+$ cells were found dispersed throughout the colonic crypt, consistent with the labeling of secretory progenitors and their progeny (Figs 4A and EV3A and B). Interestingly, while only rare fully lineage-traced crypts (< 5%) were observed at 7 days

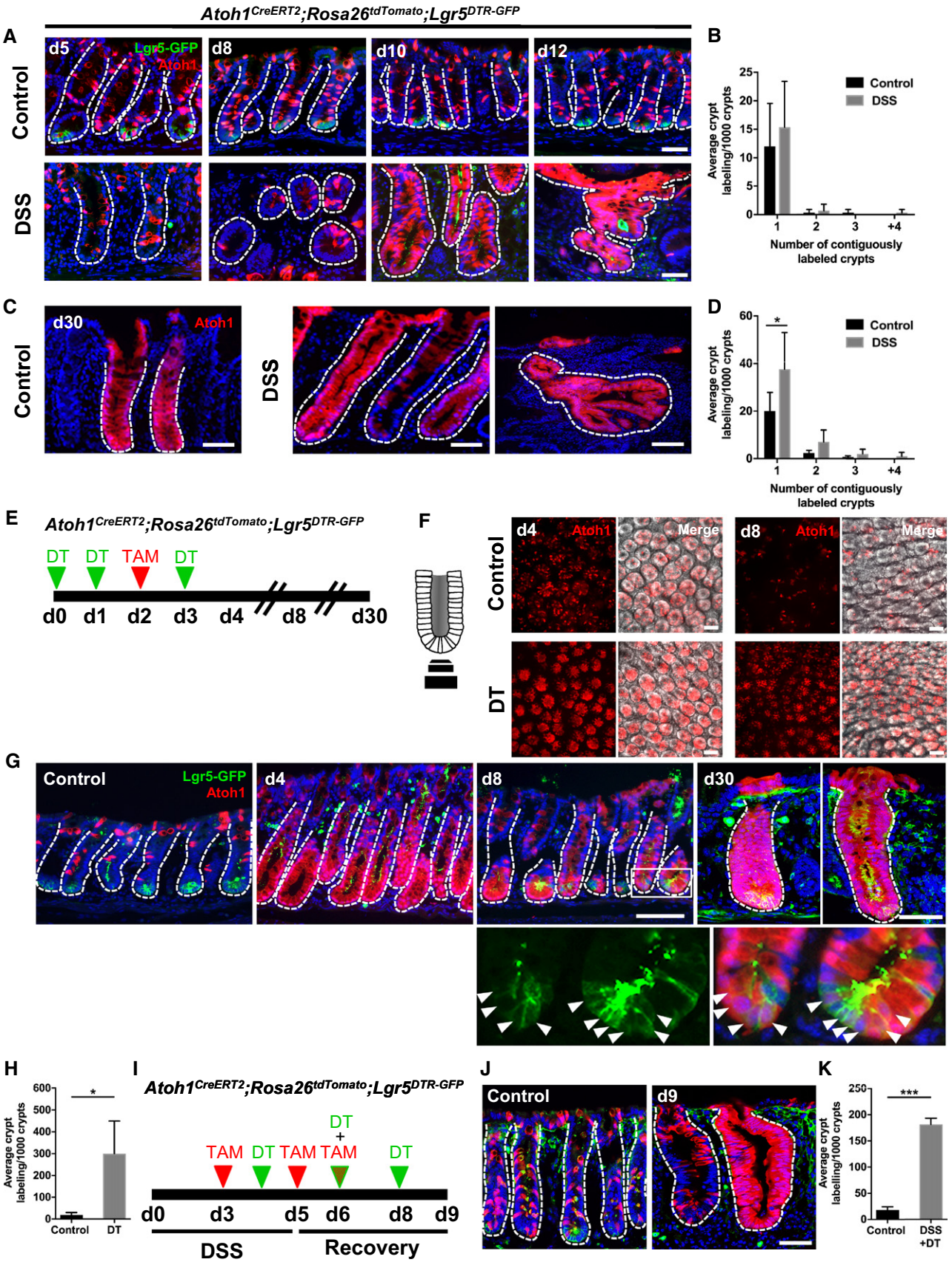
Atoh1CreERT2;Rosa26tdTomato;Lgr5DTR-GFP
A
d5
Lgr5-GFP
Atoh1
d8
d10
d12
Control
DSS
B
Control
DSS
Average crypt labeling/1000 crypts
Number of contiguously labeled crypts
C
d30
Atoh1
Control
DSS
D
Control
DSS
Average crypt labeling/1000 crypts
Number of contiguously labeled crypts
E
Atoh1CreERT2;Rosa26tdTomato;Lgr5DTR-GFP
DT DT TAM DT
d0 d1 d2 d3 d4 d8 d30
F
d4
Atoh1
Merge
d8
Atoh1
Merge
Control
DT
G
Control
Lgr5-GFP
Atoh1
d4
d8
d30
H
Average crypt labeling/1000 crypts
Control
DT
I
Atoh1CreERT2;Rosa26tdTomato;Lgr5DTR-GFP
DT + TAM DT TAM TAM DT
d0 d3 d5 d6 d8 d9
DSS
Recovery
J
Control
d9
K
Average crypt labelling/1000 crypts
Control
DSS +DT

Figure 4.

Figure 4. *Atoh1*$^+$ secretory progenitors display plasticity and contribute to colonic regeneration in homeostasis and injury.

A, B *Atoh1*$^+$ progenitors show stem cell capacity during normal homeostasis and regeneration. At early stages of recovery, d10–12, *Atoh1*$^+$ cells lineage trace the colonic crypt (N = 4 per condition).

C, D By d30 after DSS, *Atoh1*-derived stem cells continue to lineage trace complete colonic crypts (N = 4 per condition).

E Illustration of experimental protocol outlining DT treatment of *Atoh1*^{CreERT2};*ROSA26*^{tdTomato};*Lgr5*$^{DTR\text{-}GFP}$ mice.

F, G Whole mount (F) and section (G) images of *Atoh1* lineage-labeled crypts. Majority of crypts are labeled after *Lgr5*$^+$ stem cell ablation and remain label with the appearance of *Lgr5*$^+$ stem cells (inset, arrowheads). *Atoh1* lineage-labeled crypts remain by d30.

H Significantly increased labeling of crypt base was observed at d8 in DT-treated mice (N = 4 per condition).

I DSS and DT treatment of *Atoh1*^{CreERT2};*ROSA26*^{tdTomato};*Lgr5*$^{DTR\text{-}GFP}$ mice.

J, K Scattered labeling of *Atoh1*$^+$ cells in control conditions, while DSS + DT injury lead to *Atoh1* lineage-labeled crypts lacking *Lgr5*$^+$ stem cells.

Data information: Nuclei are counterstained with Dapi (blue); white dashed lines indicate basement membrane. Scale bars (A, first two panels of C, F, J) = 50 μm; scale bars (last panel of C, G) = 100 μm. Data are represented as mean ± SD analyzed using two-way ANOVA with Sidak's multiple comparisons test (B, D) and Student's t-test with Welch's correction (H, K). *$P \leq 0.05$, ***$P \leq 0.001$.

post-tamoxifen, by 30 days post-tamoxifen this increased to ~20% of total colonic crypts (Fig EV3A and B). This finding suggests that the *Atoh1*$^+$ cell population may overlap with the stem cell population during homeostasis, as previously shown in the small intestine (Kim *et al*, 2016; Ishibashi *et al*, 2018). In the setting of DSS colitis, day 12 lineage tracing of entire colonic crypts from *Atoh1*$^+$ cells remained unchanged from control mice without colitis (Fig 4A and B). *Atoh1*$^+$ cells also gave rise to newly regenerated *Lgr5*$^+$ cells 1 week post-DSS (day 12), demonstrating that *Atoh1*$^+$ progenitors are resistant to DSS colitis and contribute to the colonic epithelial regeneration (Fig 4A and B). Notably, by 30 days post-DSS, quantification of tdTomato$^+$ crypts, as a proxy of progenitor cells giving rise to multiple lineages, revealed that *Atoh1*$^+$ lineage tracing significantly increased post-colitis, consistent with the expansion of *Atoh1*$^+$ progenitors during colonic regeneration (Fig 4C and D). Taken together, our data show that *Atoh1*$^+$ progenitors can contribute to renewal during both homeostasis and injury.

To further investigate which secretory cell type is involved in *Lgr5*$^+$ cell-independent regeneration following DSS colitis, we analyzed the expression of the secretory cell markers *Prox1*, *Neurog3*, and *Bmi1* (Yan *et al*, 2017) in colonic tissue following DSS recovery by qRT–PCR. We observed increased expression of *Neurog3* and *Prox1* post-DSS at day 5 and day 19, respectively, while *Bmi1* expression remained unchanged (Fig EV2C and D). These data suggest that *Prox1*$^+$ and/or *Neurog3*$^+$ secretory cell populations may overlap with cells expressing *Atoh1,* and cells expressing either or both of these markers could be important for epithelial regeneration after injury.

To definitively distinguish between lineage tracing from *Atoh1*$^+$ progenitors and *Lgr5*$^+$ cells in the colon, we assessed *Atoh1*$^+$ lineage tracing studies in the context of *Lgr5*$^+$ cell ablation. Using *Atoh1*^{CreERT2};*ROSA26*^{tdTomato};*Lgr5*$^{DTR\text{-}GFP}$ mice, we administered DT to ablate *Lgr5*$^+$ cells while simultaneously lineage tracing from *Atoh1*$^+$ cells (Fig 4E). Our experimental paradigm effectively ablated all *Lgr5*-expressing cells from the colon, with no *Lgr5*-GFP$^+$ cells being seen in the colon 24 h following the last dose of DT (Fig 4F and G). DT ablation of *Lgr5*$^+$ cells resulted in extensive *Atoh1*$^+$ lineage labeling of crypts at day 4, followed by *Atoh1*$^+$ progenitor cell lineage tracing the colonic crypt base of nearly all crypts examined (Figs 4F–H and EV3C). This was in contrast to saline-treated controls, in which only rare *tdTomato*$^+$ crypts were detectable at day 8 post-tamoxifen, and consistent with previous reports of dedifferentiation in small intestine (Fig 4G and H; van Es *et al*, 2012; Tetteh *et al*, 2016). Indeed, tdTomato$^+$ lineage tracing significantly increased by nearly 15-fold following *Lgr5*$^+$ cell ablation compared to controls (Fig 4H). Interestingly, *Atoh1*$^+$ lineage localization at the crypt base at day 8 was correlated with the reemergence of *Lgr5*$^+$ cells and coincided with our observations in DSS colitis, where new *Lgr5*-GFP$^+$ cells derive from *Atoh1*$^+$ lineage (Fig 4G, arrowheads within inset). Further, homeostasis is maintained by *Atoh1*-derived *Lgr5*$^+$ stem cells, demonstrated by 30-day labeled crypts (Fig 4G). Remarkably, this self-renewal capacity of *Atoh1*$^+$ cells post-colitis was unaffected by simultaneous *Lgr5*$^+$ cell ablation (Fig 4I–K).

EdU labeling revealed that, at baseline, many tdTomato$^+$ *Krt19*-expressing cells within the crypt were proliferating. This was in contrast to the rare tdTomato$^+$ *Atoh1*-expressing cells which were EdU$^+$ at baseline, but more easily detectable above the crypt base by day 4 after *Lgr5*$^+$ cell ablation (Fig EV1D–F). Notably, at day 8 of *Lgr5*$^+$ cell ablation, EdU$^+$ *Atoh1*-expressing cells were seen at the crypt base (Fig EV1F). These data suggest that, unlike crypt base *Lgr5*$^+$ stem cells that are susceptible to injury, *Atoh1*$^+$ progenitor cells are located higher up within the crypt and are critical to colonic epithelial regeneration in the setting of injury.

Atoh1$^+$ colonic progenitor cells show cellular plasticity in response to injury *in vitro*

Our *in vivo* observations indicated that colonic *Atoh1*$^+$ cells have limited renewal capacity during homeostasis but show significantly increased contribution in the setting of colonic epithelial injury. Therefore, to determine whether the response of *Atoh1*$^+$ cells was intrinsic to these cells and independent of the stromal niche, we examined the behavior of *Atoh1*$^+$ cells after injury *in vitro*. First, we isolated colonic epithelial cells from *Atoh1*^{CreERT2};*ROSA26*^{tdTomato} mice to generate colonic organoids. Then, using 4-hydroxytamoxifen (4-OHT), we induced recombination in organoids and compared the contribution of *Atoh1*-tdTomato$^+$ cells under control conditions or following 4 Gy of irradiation (Fig 5A). We could not detect any tdTomato fully labeled colonic organoids up to 12 days after initial culture (pre-passage). However, following 4 Gy of irradiation, we observed a significant expansion of *Atoh1*-derived tdTomato$^+$ cells by day 12 (Fig 5B and C), indicating that *in vitro*, *Atoh1*$^+$ progenitors display cellular plasticity and contribute to epithelial regeneration in the setting of injury. The expansion of *Atoh1*$^+$ cells was similarly evident upon irradiation of small intestinal organoids, confirming that *Atoh1*$^+$ secretory progenitors in small intestinal organoids display plasticity comparable to colonic organoids

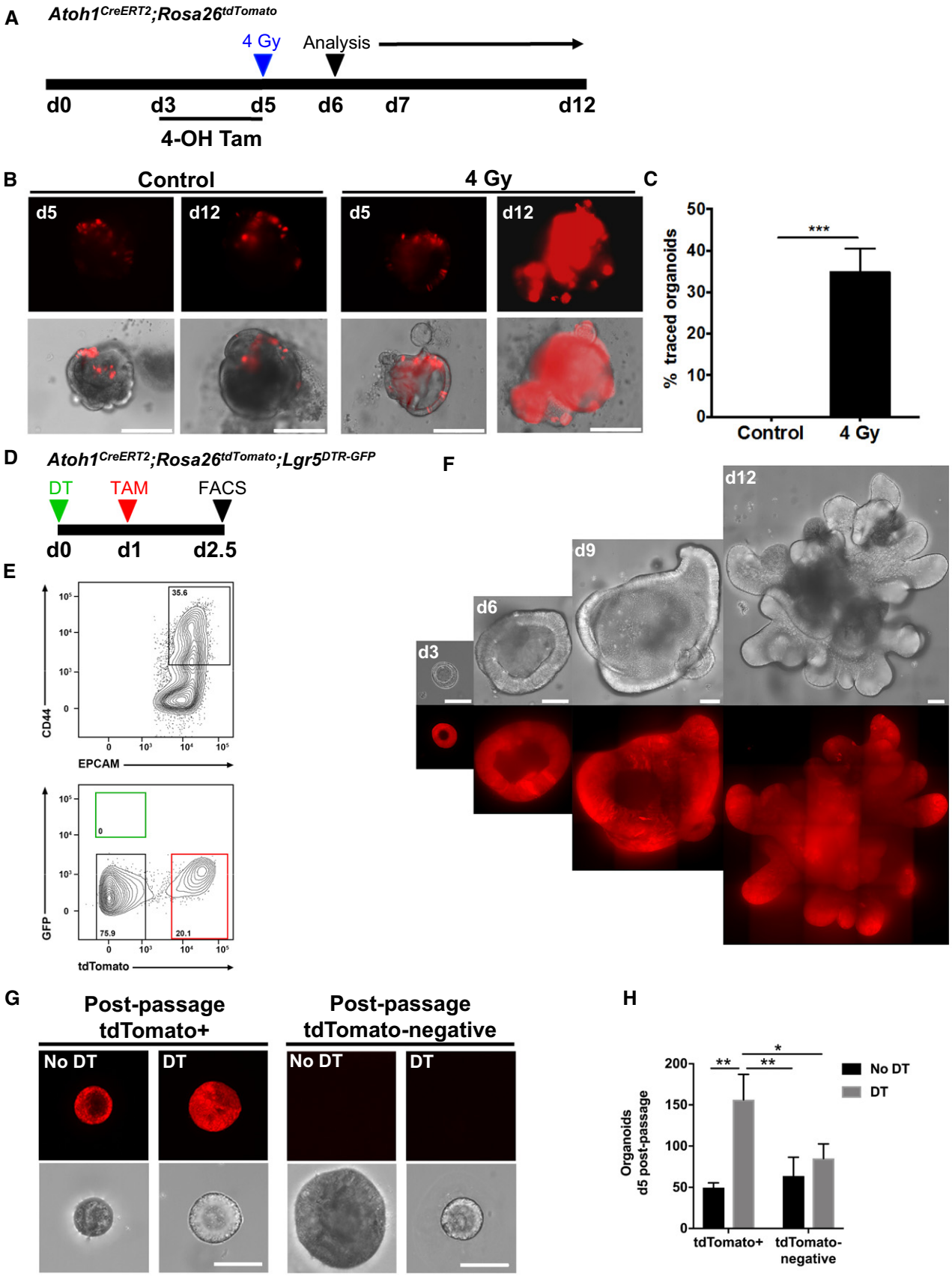
A
Atoh1CreERT2;Rosa26tdTomato
4 Gy
Analysis
d0
d3
d5
d6
d7
d12
4-OH Tam
B
Control
4 Gy
d5
d12
C
% traced organoids
***
Control
4 Gy
D
Atoh1CreERT2;Rosa26tdTomato;Lgr5DTR-GFP
DT
TAM
FACS
d0
d1
d2.5
E
CD44
EPCAM
35.6
GFP
tdTomato
75.9
20.1
F
d3
d6
d9
d12
G
Post-passage tdTomato+
Post-passage tdTomato-negative
No DT
DT
H
Organoids d5 post-passage
No DT
DT
tdTomato+
tdTomato-negative

Figure 5.

Figure 5. *Atoh1*$^+$ colonic progenitor cells show renewal capacity *in vitro* upon injury.

A Illustration of experimental protocol outlining 4-OHT induction and irradiation of *Atoh1*^{CreERT2};*ROSA26*^{tdTomato} colonic organoids.

B, C Sporadic labeling of *Atoh1*$^+$ cells after 4-OHT induction. Following irradiation, entire colonic organoids exhibit full lineage labeling of *Atoh1*$^+$ cells, characteristic of multipotent stem cells (N = 3 per condition).

D, E Flow cytometry for tdTomato$^+$ cells in crypt epithelium from DT-treated *Atoh1*^{CreERT2};*Lgr5*$^{DTR\text{-}GFP}$;*ROSA26*^{tdTomato} mice.

F tdTomato$^+$ colonic organoids from single *Atoh1*-tdTomato$^+$/*Lgr5*-negative cells (N = 1; n = 3 technical replicates per condition).

G Post-passage colonic organoids established from single tdTomato$^+$cells of control or DT-treated mice continue growing. tdTomato-negative cells of control or DT-treated mice also form colonic organoids after passaging.

H tdTomato$^+$ colonic organoids established from single cells from mice in which *Lgr5*$^+$ stem cells have been ablated show higher growth efficiency compared to their colonic organoid counterparts (N = 1; n = 3 technical replicates per condition).

Data information: Scale bars (B, F) = 100 μm; scale bars (G) = 50 μm. Data are represented as mean ± SD analyzed using Student's t-test (C) and mean ± SD analyzed using two-way ANOVA with Sidak's multiple comparisons test (H). *$P \leq 0.05$, **$P \leq 0.01$, ***$P \leq 0.001$.

(Fig EV4A–C). We observed a similar phenomenon following mechanical stress induced by passaging of organoids (Sambuy *et al*, 2005; Dupont *et al*, 2011; Zachos *et al*, 2016), such that by days 14–15 *Atoh1*-derived tdTomato$^+$ cells in small intestinal (Fig EV4D–F) and colonic (Fig EV5A–C) organoids had undergone a significant expansion. This was in striking contrast to initial culture of small intestinal and colonic organoids, in which there was a gradual decrease in the number of tdTomato$^+$ cells over time, consistent with the labeling of short-lived progenitors and/or secretory cells (Figs EV4E and EV5B). Indeed, tdTomato$^+$ cells gradually disappeared prior to organoid passage.

Next, to test whether *Atoh1*$^+$ cells in the colon have renewal capacity *in vitro*, we carried out single cell organoid cultures, as previously described (Sato *et al*, 2009). Using *Atoh1*^{CreERT2};*ROSA26*^{tdTomato};*Lgr5*$^{DTR\text{-}GFP}$ mice treated with tamoxifen, we dissociated colonic epithelia into single cells and isolated tdTomato$^+$ cells by flow cytometry (FACS; Fig 5D and E). We then seeded 10^4 single *Atoh1*-expressing tdTomato$^+$ cells per well and found that *Atoh1*$^+$ cells displayed the capacity to form colonic organoids (Fig 5F), as did occasional tdTomato-negative cells. We then compared colonic organoid formation as a measure of stem cell capacity of *Atoh1*$^+$ or *Atoh1*-negative crypt cells from DT-treated and control mice and found significantly increased colonic organoid formation of *Atoh1*$^+$ cells after *Lgr5*$^+$ stem cell ablation (Fig 5G and H). Taken together, these data demonstrate that, whereas *Atoh1*$^+$ secretory cells show infrequent renewal capacity during normal homeostasis, they have a significantly increased capacity to renew the epithelium and dedifferentiate to stem cells upon injury or ablation of the *Lgr5*-expressing stem cells.

Atoh1$^+$ colonic progenitor cells are essential for epithelial regeneration post-injury

Given our observation that *Atoh1*$^+$ secretory progenitors display renewal capacity in the setting of colonic epithelial injury, we next set out to determine whether *Atoh1*$^+$ cells are dispensable for colonic regeneration in colitis. To examine this, we crossed *Atoh1*^{CreERT2};*ROSA26*^{tdTomato} with *ROSA26*^{DTR} mice, which allowed us to conditionally and selectively ablate *Atoh1*-expressing cells upon treatment with DT. Following the protocol outlined in Fig 6A, we examined the effects of *Atoh1*$^+$ cell ablation in the setting of DSS colitis in *Atoh1*^{CreERT2};*ROSA26*$^{tdTomato/DTR}$ mice. Using tdTomato$^+$ cells as a surrogate marker of Cre-induced DTR expression in *Atoh1*-expressing cells, we observed that following DT treatment, *Atoh1*-tdTomato$^+$ cell lineage tracing was only marginally decreased by day 12 (Fig 6B), which may be the result of higher sensitivity of *ROSA26*^{tdTomato} to recombination than the *ROSA26*^{DTR} allele. Nevertheless, concurrent *Atoh1*$^+$ cell ablation with DSS colitis resulted in exacerbation of colitis as seen by significantly increased weight loss and decreased mouse survival by day 9 (Fig 6C). Moreover, *Atoh1*$^+$ cell ablation resulted in significantly increased histologic damage (Fig 6D, arrow and E), indicating that *Atoh1*$^+$ cells play an important functional role in epithelial regeneration after colitis.

To further test whether *Atoh1*$^+$ cells are required for epithelial regeneration post-injury, we isolated colonic epithelial cells from *Atoh1*^{CreERT2};*ROSA26*$^{tdTomato/DTR}$ mice and generated colonic organoids. Following 4-OHT induction of organoids to lineage label *Atoh1*$^+$ cells (Fig 6F), we determined that DT effectively ablated *Atoh1*$^+$ cells *in vitro*, as seen by a significant reduction in tdTomato$^+$ cells at day 2 post-DT (Fig 6G and H). To then examine the effect of *Atoh1*$^+$ cell ablation in the setting of injury, we subjected the organoids to 4 Gy irradiation (Fig 6F). As we previously demonstrated, *Atoh1*$^+$ cells exhibit self-renewal capacity and expand to give rise to entire organoids in the setting of radiation injury. However, the combination of irradiation and DT-induced *Atoh1*$^+$ cell ablation resulted in impaired regenerative capacity and ultimately colonic organoid death, in contrast to saline-treated control colonic organoids (Fig 6I and J). These data demonstrate that *Atoh1*$^+$ cell renewal capacity is required for the regenerative capacity of the colonic epithelium after injury affecting *Lgr5*$^+$ stem cells.

Discussion

It is broadly accepted that *Lgr5*$^+$ stem cells at the crypt base maintain epithelial turnover during homeostasis. Upon epithelial insult, however, *Lgr5*$^+$ cells are susceptible to injury, and they must be regenerated before homeostasis can resume. In the small intestine, this renewal can occur through dedifferentiation of committed cells and perhaps from a population of reserve stem cells that have been suggested to reside higher up within the intestinal crypt (Li & Clevers, 2010; Yan *et al*, 2012; Barker, 2014; Asfaha *et al*, 2015). Furthermore, in the small intestine, newly formed *Lgr5*$^+$ cells are indispensable for regeneration following radiation injury (Metcalfe *et al*, 2014). In contrast, following DSS-induced colonic injury, DT ablation of colonic *Lgr5*$^+$ stem cells in *Lgr5*^{DTR} mice has no apparent effect on regeneration (Metcalfe *et al*, 2014). Additionally, colonic epithelial injury resulting in *Lgr5*$^+$ stem cell disruption promotes crypt hyperplasia and hyperproliferation. Together, these data suggest that colonic *Lgr5*$^+$ stem cells are dispensable for epithelial

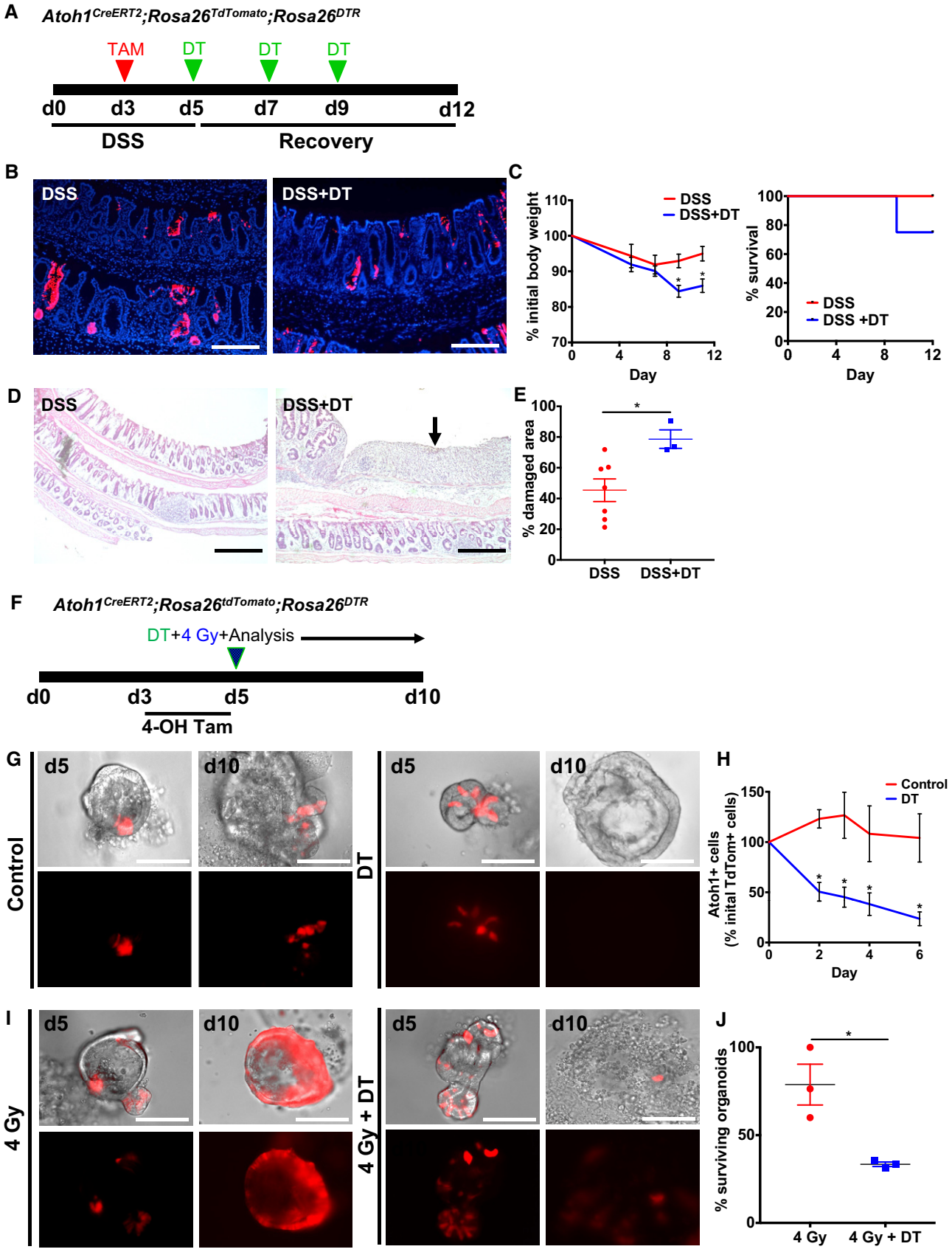

Figure 6.

Figure 6. *Atoh1*$^+$ colonic progenitor cells are essential for epithelial regeneration post-injury.

A Illustration of experimental protocol outlining DSS-induced colitis in *Atoh1*^{CreERT2};*ROSA26*$^{tdTomat/DTR}$ mice.

B *Atoh1*$^+$ lineage labeling post-DSS and DSS + DT.

C DSS + DT-treated mice exhibit significant weight loss and lower survival compared to DSS alone (N = 4–7 control; N = 3–4 DSS).

D, E Hematoxylin and eosin staining of colonic epithelium after DSS versus DSS + DT (D). Extensive epithelial damage was observed (D, arrow) and quantified in DSS + DT-treated mice (N = 7 control; N = 4 DSS).

F Illustration of experimental protocol outlining 4-OHT induction and irradiation in *Atoh1*^{CreERT2};*ROSA26*$^{tdTomato/DTR}$ colonic organoids.

G, H DT treatment effectively ablates *Atoh1*$^+$ cells shown by reduced number of tdTomato$^+$ cells per organoid.

I, J Concurrent irradiation injury and *Atoh1*$^+$ cell ablation result in significantly reduced organoid survival (N = 3; n = 3 technical replicates per condition).

Data information: Scale bars (B) = 200 μm; scale bars (D) = 400 μm; scale bars (G, I) = 100 μm. Data are represented as mean ± SEM analyzed using Student's t-test. *$P \leq 0.05$.

regeneration and that epithelial repair can be fueled by an *Lgr5*-negative cell population. In order to further delineate which cell population is the principal contributor to colonic epithelial regeneration, we used genetic fate-mapping mouse models to examine the role of secretory and absorptive progenitor cells following injury.

Using an allele that labels *Krt19*-expressing cells, including progenitors and stem cells that are *Lgr5*-negative (Asfaha *et al*, 2015), we determined that a cell population distinct from *Lgr5*$^+$ stem cells contributes to colonic epithelial regeneration post-colitis. Notably, *Lgr5*-negative, *Krt19*-expressing cells are required for proper colonic regeneration to occur, as ablation of *Krt19*$^+$ cells results in impaired colonic regeneration. These findings are consistent with previous reports in the small intestine showing that plasticity of secretory and absorptive lineages contributes to epithelial regeneration when *Lgr5*$^+$ stem cells are injured (van Es *et al*, 2012; Tetteh *et al*, 2016; Yan *et al*, 2017). These data confirm that an *Lgr5*-negative cell within the colonic crypt has the capacity to revert to a stem cell state to regenerate all epithelial cells, including *Lgr5*$^+$ cells.

To more precisely define the subset of *Lgr5*-negative cells that contribute to colonic regeneration, we examined the fate of *Notch1*$^+$ absorptive and *Atoh1*$^+$ secretory progenitors following colitis. Our findings demonstrate that *Notch1*$^+$ absorptive progenitors do not play a role in colonic epithelial repair, whereas *Atoh1*$^+$ secretory cells proliferate and expand to contribute to epithelial regeneration during colitis. Interestingly, in the colon, *Atoh1*$^+$ secretory cells also show infrequent renewal capacity during normal homeostasis, in contrast to the small intestine, in which *Atoh1*$^+$ secretory cells do not lineage trace at baseline. Upon injury, however, both colonic and intestinal *Atoh1*$^+$ cells expand to renew the epithelium, consistent with plasticity required for crypt regeneration. Our observations are consistent with the recent findings reported by two other groups demonstrating that *Atoh1*$^+$ secretory cells are able to contribute to colonic regeneration post-colitis (Ishibashi *et al*, 2018; Tomic *et al*, 2018). Thus, a subset of *Atoh1*$^+$ cells in the colon can renew the epithelium during normal homeostasis, whereas in the small intestine, *Atoh1*$^+$ cells behave similarly to intestinal *Dll1*$^+$ progenitors cells that are short-lived and only lineage trace upon epithelial injury (van Es *et al*, 2012).

Complementing the recent findings showing that phosphorylation of ATOH1 regulates the plasticity of secretory progenitors (Tomic *et al*, 2018), we found that renewal by *Atoh1*$^+$ cells is independent of *Lgr5*$^+$ stem cells and that *Atoh1*$^+$ cells are multipotent in terms of their renewal capacity. This is demonstrated by their ability to give rise to colonic organoids *in vitro*, as well as to lineage trace *in vivo* in the absence of *Lgr5*$^+$ cells by DT ablation during regeneration. Overall, our results support the idea that during colonic regeneration, *Atoh1*$^+$ progenitors undergo a proliferative phase 4 days post-injury, which takes place in complete absence of the bona fide *Lgr5*$^+$ stem cells. Subsequently, *Atoh1*$^+$ cells enter a normalization phase ~8 days post-injury, characterized by reemergence of *Lgr5*$^+$ stem cells and resumption of steady state. A similar phenomenon is also seen in intestinal regeneration after irradiation (Kim *et al*, 2017).

Notably, *Atoh1*-negative cells formed colonic organoids in the absence of *Lgr5*$^+$ cells, albeit to a smaller degree than *Atoh1*$^+$ cells. This suggests that, in the context of injury, the presence of additional cells within the crypt may also aid in colonic regeneration, as we and others have recently proposed (Yui *et al*, 2018). Importantly, we demonstrate for the first time that *Atoh1*$^+$ cells are essential for colonic regeneration, as their ablation during colitis significantly impairs colonic healing. Moreover, our data also shows that the combination of radiation or DSS colitis plus *Atoh1*$^+$ cell ablation significantly impairs colonic healing, thus suggesting that simultaneous elimination of both *Lgr5*$^+$ and *Atoh1*$^+$ cell populations is detrimental to colonic healing.

In summary, we have found that the renewal capacity of *Atoh1*$^+$ secretory progenitors, which is modest during normal homeostasis, is critical for colonic epithelial regeneration during colitis. Importantly, colonic regeneration in this context is independent of *Lgr5*$^+$ stem cells, and *Notch1*$^+$ absorptive progenitors do not significantly contribute to this process. These findings suggest that future therapy aimed at promoting colonic regeneration in colitis may be enhanced by promoting the survival and function of *Atoh1*$^+$ secretory progenitors.

Materials and Methods

Animals

Mouse lines used include combinations of the following alleles or transgenes: *Lgr5*$^{GFP\text{-}IRES\text{-}CreERT2}$ (Jax 008875; Barker *et al*, 2007), *Lgr5*$^{DTR\text{-}GFP}$ (Tian *et al*, 2011), *Krt19*$^{BAC\text{-}CreERT2}$ (Asfaha *et al*, 2015), *Notch1*^{CreERT2} (Fre *et al*, 2011), *Atoh1*^{CreERT2} (Fujiyama *et al*, 2009), *ROSA26*^{DTR} (Jax 007900; Buch *et al*, 2005), and *ROSA26*^{tdTomato} (Jax 007905; Madisen *et al*, 2010). Mice were 8–16 weeks of age at the start of each experiment. Rodent work was done in accordance with approved protocols by the Institutional Animal Care and Use Committees at University of California San Francisco and University of Western Ontario.

DSS-induced colitis and tamoxifen induction

Mice were exposed to 2.5–3% (w/v) DSS (DS1004, Gojira Fine Chemicals or 02160110, MP Biomedicals) in their drinking water for 5 days (D0–D5). The mice were closely monitored during the treatment and recovery periods using body weight and other established criteria. Mice were oral gavaged with three doses of 1–6 mg tamoxifen (0215673894, MP Biomedicals or T5648, Sigma) dissolved in corn oil, and colonic tissue was harvested at the indicated time points during recovery.

Diphtheria toxin cell ablation

Using the *Lgr5*$^{DTR\text{-}GFP}$ allele, the diphtheria toxin receptor is constitutively expressed in all *Lgr5*-expressing cells. For ablation studies, mice were treated with 200–1,000 ng of diphtheria toxin (322326, Sigma-Aldrich) at regular intervals and monitored as described above. Using *Atoh1*^{CreERT2};*ROSA26*^{DTR} mice, we are able to conditionally express the diphtheria toxin receptor in Atoh1-expressing cells upon tamoxifen treatment. For ablation studies *in vivo*, mice were treated with 1,000 ng of diphtheria toxin at regular intervals and monitored as described above. For treatment of organoids *in vitro*, diphtheria toxin was added to the culture medium at a final concentration of 200 ng/ml every other day.

Tissue preparation for immunofluorescence and histology

Harvested intestinal and colonic tissues were perfusion-fixed or fresh-frozen. For perfusion fixation, animals were anesthetized by intraperitoneal (i.p.) injection of 250 mg/kg of body weight avertin (2,2,2-tribromoethanol) and transcardially perfused with 4% paraformaldehyde (PFA) in 0.1 M phosphate-buffered saline (PBS). Dissected tissues were post-fixed in 4% PFA for 3 h at 4°C and cryoprotected in 30% sucrose in 1× PBS overnight at 4°C. Tissue was embedded in OCT compound (4583, Sakura or 23-730-571, Thermo Fisher Scientific), frozen, and stored at −80°C. Fresh tissues were rinsed in sterile ice-cold 1× phosphate-buffered saline (PBS), embedded in OCT compound, frozen, and stored at −80°C. Fresh tissue sections were fixed with 4% paraformaldehyde. For paraffin-embedded tissues, we fixed tissues with 4% paraformaldehyde for 24–48 h, followed by paraffin processing, using a standard protocol.

Immunofluorescence and histology

Immunofluorescence was performed on 6- to 7-μm cryosections. Primary antibodies and dilutions used are as follows: chicken anti-GFP (1:1,000; GFP-1020, Aves Labs), rabbit anti-DCLK1 (1:200; ab31704, Abcam), rabbit anti-chromogranin A (1:100; 20085, ImmunoStar), and rabbit anti-Muc2 (1:100; ab76774, Abcam). Appropriate secondary antibodies from Thermo Fisher Scientific were used at 1:1,000. Sections were counterstained with Dapi (1:10,000; D9542, Sigma) and coverslipped with Vectashield (H-1000, Vector Labs) or ProLong Gold Antifade (P36930, Thermo Fisher Scientific). For histology assessment, 6- to 7-μm paraffin or frozen sections were prepared and stained with hematoxylin and eosin using standard methods. Slides were coverslipped using Permount (SP15-100, Fisher Scientific).

Tissue preparation for RNAscope

Intestinal and colonic tissues were immersed in 4% PFA for 24 h at room temperature, followed by standard dehydration and paraffin embedding.

RNAscope and quantification of *Lgr5* transcripts

RNA *in situ* hybridization for *Lgr5* expression was performed on 7-μm paraffin sections using RNAscope® 2.5 High Definition (HD)—Red Assay (322350, Advanced Cell Diagnostics). Manufacturer's protocol was followed with 15 min of target retrieval and 30 min of protease digestion, using the following probe: Mm *Lgr5* (312171, Advanced Cell Diagnostics). Quantification of *Lgr5* mRNA transcripts was performed using the open-source platform Fiji (Schindelin *et al*, 2012) and the analysis guidelines from Advanced Cell Diagnostics. Area of single probes was measured and used to determine total probe count within probe clusters. Total probe clusters containing at least 10 probes were quantified and normalized to number of crypts analyzed in proximal, mid, and distal colon.

Intestinal and colonic organoid cultures

Intestinal or colonic crypts were isolated from mouse as previously described by Bjerknes and Cheng with some modifications, and cultured in the presence of EGF 50 ng/ml (PMG8043, Invitrogen), mNoggin 100 ng/ml (250-38, PeproTech), R-spondin 1 μg/ml, and Wnt3a 100 ng/ml (315-20, PeproTech) for colonic cultures, as previously described (Sato *et al*, 2009). Organoids were treated with 4-hydroxytamoxifen (4-OHT) 1 μM (H6278, Sigma) to induce Cre-recombinase activity. Organoids were irradiated using a Cobalt-60 Irradiator (Gammacell) at 80.3 cGy/min for a total dose of 4 Gy. Traced organoids were quantified as the percentage of organoids displaying entire tdTomato$^+$ crypt tracing over the total number of organoids with detectable *Atoh1*-tdTomato$^+$ cells per well.

Single cell colonic organoid cultures

Flow cytometry

Colon from *Atoh1*^{CreERT2};*ROSA26*^{tdTomato};*Lgr5*$^{DTR\text{-}GFP}$ mice was dissected, flushed with cold 1× PBS, opened lengthwise, and subjected to 10 mM DTT in complete HBSS (14185-020, Gibco; HBSS, 10 mM HEPES pH 8, 2% FBS) at 37°C for 20 min followed by 10-min wash in complete HBSS. Next, colonic tissue was cut into 0.5-mm pieces and subjected to 10 mM EDTA in complete HBSS. After EDTA incubation, the solution was subjected to vigorous mechanical dissociation. The suspension was filtered through a 40-μm cell strainer, the volume was adjusted to 45 ml with cold RPMI (10-543Q, Lonza), and cells were pelleted by centrifugation at 350 × *g* for 5 min. The resulting cell pellet was resuspended in complete HBSS containing 5 mM EDTA and stained for flow cytometry using CD45-BV605 (30-F11, 103139, BioLegend), CD326/EpCAM-APC (G8.8, 118213, BioLegend), and CD44-PeCy7 (IM7, 103029, BioLegend) for 30 min on ice. After washing, Dapi (1:10,000; D9542, Sigma) was added. Cells were subsequently sorted on a FACSAria II (BD Bioscience) cell sorter into 500 μl

advanced DMEM/F12 medium (12634-010, Thermo Fisher Scientific) supplemented with 1% GlutaMAX (35050061, Thermo Fisher Scientific) and 1% penicillin/streptomycin (15140148, Thermo Fisher Scientific).

Culture

Cells were spun down and resuspended in 50 µl Phenol-free Matrigel (356231, Cornig) supplemented with 10 µM Jagged-1 (188-204, Anaspec,), 500 ng/ml human EGF (AF-100-15, PeproTech), 1 µg/ml murine Noggin (250-38, PeproTech), 10% mouse R-spondin1 conditioned medium (gift of Noah Shroyer, Baylor College of Medicine), and 10% murine Wnt3a conditioned medium (CRL-2647, ATCC). Matrigel drops of 50 µl were plated in a 12-well cell culture plate and left to set at 37°C for 15 min. Organoids were cultured in advanced DMEM/F12 in the presence of 50 ng/ml human EGF, 100 ng/ml murine Noggin, 5% mouse R-spondin1 conditioned medium, 50% murine Wnt3a conditioned medium, 10 mM nicotinamide (N3376, Sigma), 1% N-2 supplement (17502048, Thermo Fisher Scientific), and 2% B-27 supplement (17504044, Thermo Fisher Scientific). During first 3 days of culture, 2.5 µM Y-27632 dihydrochloride (Y0503, Sigma), 2.5 µM Chir99021 (SML1046, Sigma), and 1 µM Jagged-1 were used, and medium was changed every 3 days.

Image acquisition and analysis

Fluorescence and bright-field images were acquired using a Leica DM5000 B and Leica DFC 500 with LAS V4.9 software or EVOS-FL Auto microscope. Confocal images were obtained as a *z*-stack of 0.76-µm optical sections acquired sequentially using a Leica TCS SP5 II confocal microscope with LAS X software. Ventral images of whole mount crypts were acquired with a Zeiss Observer Z1 with ZEN blue software.

To determine the severity of colitis, mouse body weight and survival were assessed during the experimental time course. Furthermore, colonic tissue was examined for percentage of damaged area. Assessment of damage throughout the entire length of the colon was made possible using cross section through the colonic Swiss roll preparation. Total colonic area and total damaged area were obtained using EVOS FL Auto area detection software (Life Technologies), and total damaged area was expressed as a percentage of total colonic area. The number of contiguously labeled crypts was used as a determinant of tissue regeneration and was obtained by manually counting the number of contiguously lineage-traced crypts and expressing these values per 1,000 crypts.

Statistical analysis

Normally distributed data were analyzed using parametric tests including two-tailed Student's *t*-test with Welch's correction, one-way ANOVA with Bonferroni correction, or two-way ANOVA with Sidak's multiple comparisons test. The non-parametric Mann–Whitney *U*-test was used if the data did not fit a normal distribution. Significance was taken as $P < 0.05$ with a confidence interval of 95%. Data are presented as mean ± SD for parametric data or as mean ± SEM for non-parametric data.

Expanded View for this article is available online.

Acknowledgements

We thank Nicholas Wang, Asoka Rathnayake, and Liyue Zhang for technical assistance and Drs. Ysbrand M. Nusse, Jimmy Kuang-Hsien Hu, Amnon Sharir and Kara L. McKinley for helpful discussions. This work was supported by operating grants from CIHR and Cancer Research Society awarded to S.A. and by the National Institutes of Health (R35-DE026602, U01-DK103147) and the California Institute for Regenerative Medicine (RN3-06525) to O.D.K. Research reported in this publication was supported by National Institute of Diabetes and Digestive and Kidney Disorders (NIDDK) and National Institute of Allergy and Infectious Diseases (NIAID) of the National Institutes of Health under grant number U01DK103147. The content is solely the responsibility of the authors and does not necessarily represent the official views of the National Institutes of Health. E.F. was supported by a Cancer Research and Technology Transfer (CaRTT) Strategic Training Program Stipend, and H.G. was supported in part by a studentship from the Lawson Internal Research Fund.

Author contributions

Conceptualization: DC-A, ENF, RN, HJG, ODK, SA; Methodology and data acquisition: DC-A, ENF, RN, HJG, TW, MAP, ODK, SA; Analysis: DC-A, ENF, RN, HJG, ODK, SA; Investigation: DC-A, ENF, RN, HJG, FJdS, ODK, SA; Writing: DC-A, ENF, HJG, ODK, SA.

Conflict of interest

F.J.d.S. is an employee of Genentech and owns shares in Roche.

References

Asfaha S, Hayakawa Y, Muley A, Stokes S, Graham TA, Ericksen RE, Westphalen CB, von Burstin J, Mastracci TL, Worthley DL, Guha C, Quante M, Rustgi AK, Wang TC (2015) Krt19(+)/Lgr5(-) cells are radioresistant cancer-initiating stem cells in the colon and intestine. *Cell Stem Cell* 16: 627 – 638

Barker N, van Es JH, Kuipers J, Kujala P, van den Born M, Cozijnsen M, Haegebarth A, Korving J, Begthel H, Peters PJ, Clevers H (2007) Identification of stem cells in small intestine and colon by marker gene Lgr5. *Nature* 449: 1003 – 1007

Barker N, Clevers H (2010) Leucine-rich repeat-containing G-protein-coupled receptors as markers of adult stem cells. *Gastroenterology* 138: 1681 – 1696

Barker N (2014) Adult intestinal stem cells: critical drivers of epithelial homeostasis and regeneration. *Nat Rev Mol Cell Biol* 15: 19 – 33

Barriga FM, Montagni E, Mana M, Mendez-Lago M, Hernando-Momblona X, Sevillano M, Guillaumet-Adkins A, Rodriguez-Esteban G, Buczacki SJA, Gut M, Heyn H, Winton DJ, Yilmaz OH, Attolini CS, Gut I, Batlle E (2017) Mex3a marks a slowly dividing subpopulation of Lgr5+ intestinal stem cells. *Cell Stem Cell* 20: 801 – 816 e807

Buch T, Heppner FL, Tertilt C, Heinen TJAJ, Kremer M, Wunderlich FT, Jung S, Waisman A (2005) A Cre-inducible diphtheria toxin receptor mediates cell lineage ablation after toxin administration. *Nature Methods* 2: 419 – 426

Buczacki SJ, Zecchini HI, Nicholson AM, Russell R, Vermeulen L, Kemp R, Winton DJ (2013) Intestinal label-retaining cells are secretory precursors expressing Lgr5. *Nature* 495: 65 – 69

Cooper HS, Murthy SN, Shah RS, Sedergran DJ (1993) Clinicopathologic study of dextran sulfate sodium experimental murine colitis. *Lab Invest* 69: 238 – 249

Davidson LA, Goldsby JS, Callaway ES, Shah MS, Barker N, Chapkin RS (2012) Alteration of colonic stem cell gene signatures during the regenerative response to injury. *Biochem Biophys Acta* 1822: 1600 – 1607

Dupont S, Morsut L, Aragona M, Enzo E, Giulitti S, Cordenonsi M, Zanconato F, Le Digabel J, Forcato M, Bicciato S, Elvassore N, Piccolo S (2011) Role of YAP/TAZ in mechanotransduction. *Nature* 474: 179 – 183

van Es JH, van Gijn ME, Riccio O, van den Born M, Vooijs M, Begthel H, Cozijnsen M, Robine S, Winton DJ, Radtke F, Clevers H (2005) Notch/gamma-secretase inhibition turns proliferative cells in intestinal crypts and adenomas into goblet cells. *Nature* 435: 959 – 963

van Es JH, Sato T, van de Wetering M, Lyubimova A, Nee AN, Gregorieff A, Sasaki N, Zeinstra L, van den Born M, Korving J, Martens AC, Barker N, van Oudenaarden A, Clevers H (2012) Dll1+ secretory progenitor cells revert to stem cells upon crypt damage. *Nat Cell Biol* 14: 1099 – 1104

Fre S, Hannezo E, Sale S, Huyghe M, Lafkas D, Kissel H, Louvi A, Greve J, Louvard D, Artavanis-Tsakonas S (2011) Notch lineages and activity in intestinal stem cells determined by a new set of knock-in mice. *PLoS One* 6: e25785

Fujiyama T, Yamada M, Terao M, Terashima T, Hioki H, Inoue YU, Inoue T, Masuyama N, Obata K, Yanagawa Y, Kawaguchi Y, Nabeshima Y, Hoshino M (2009) Inhibitory and excitatory subtypes of cochlear nucleus neurons are defined by distinct bHLH transcription factors, Ptf1a and Atoh1. *Development* 136: 2049 – 2058

Furuyama K, Kawaguchi Y, Akiyama H, Horiguchi M, Kodama S, Kuhara T, Hosokawa S, Elbahrawy A, Soeda T, Koizumi M, Masui T, Kawaguchi M, Takaori K, Doi R, Nishi E, Kakinoki R, Deng JM, Behringer RR, Nakamura T, Uemoto S (2011) Continuous cell supply from a Sox9-expressing progenitor zone in adult liver, exocrine pancreas and intestine. *Nat Genet* 43: 34 – 41

Hirata A, Utikal J, Yamashita S, Aoki H, Watanabe A, Yamamoto T, Okano H, Bardeesy N, Kunisada T, Ushijima T, Hara A, Jaenisch R, Hochedlinger K, Yamada Y (2013) Dose-dependent roles for canonical Wnt signalling in *de novo* crypt formation and cell cycle properties of the colonic epithelium. *Development* 140: 66 – 75

Ishibashi F, Shimizu H, Nakata T, Fujii S, Suzuki K, Kawamoto A, Anzai S, Kuno R, Nagata S, Ito G, Murano T, Mizutani T, Oshima S, Tsuchiya K, Nakamura T, Watanabe M, Okamoto R (2018) Contribution of ATOH1(+) cells to the homeostasis, repair, and tumorigenesis of the colonic epithelium. *Stem Cell Reports* 10: 27 – 42

Itzkovitz S, Lyubimova A, Blat IC, Maynard M, van Es J, Lees J, Jacks T, Clevers H, van Oudenaarden A (2012) Single-molecule transcript counting of stem-cell markers in the mouse intestine. *Nat Cell Biol* 14: 106 – 114

Kim TH, Saadatpour A, Guo G, Saxena M, Cavazza A, Desai N, Jadhav U, Jiang L, Rivera MN, Orkin SH, Yuan GC, Shivdasani RA (2016) Single-cell transcript profiles reveal multilineage priming in early progenitors derived from Lgr5(+) intestinal stem cells. *Cell Rep* 16: 2053 – 2060

Kim CK, Yang VW, Bialkowska AB (2017) The role of intestinal stem cells in epithelial regeneration following radiation-induced gut injury. *Curr Stem Cell Rep* 3: 320 – 332

Laroui H, Ingersoll SA, Liu HC, Baker MT, Ayyadurai S, Charania MA, Laroui F, Yan Y, Sitaraman SV, Merlin D (2012) Dextran sodium sulfate (DSS) induces colitis in mice by forming nano-lipocomplexes with medium-chain-length fatty acids in the colon. *PLoS One* 7: e32084

Li L, Clevers H (2010) Coexistence of quiescent and active adult stem cells in mammals. *Science* 327: 542 – 545

Madisen L, Zwingman TA, Sunkin SM, Oh SW, Zariwala HA, Gu H, Ng LL, Palmiter RD, Hawrylycz MJ, Jones AR, Lein ES, Zeng H (2010) A robust and high-throughput Cre reporting and characterization system for the whole mouse brain. *Nat Neurosci* 13: 133 – 140

Metcalfe C, Kljavin NM, Ybarra R, de Sauvage FJ (2014) Lgr5+ stem cells are indispensable for radiation-induced intestinal regeneration. *Cell Stem Cell* 14: 149 – 159

Montgomery RK, Carlone DL, Richmond CA, Farilla L, Kranendonk ME, Henderson DE, Baffour-Awuah NY, Ambruzs DM, Fogli LK, Algra S, Breault DT (2011) Mouse telomerase reverse transcriptase (mTert) expression marks slowly cycling intestinal stem cells. *Proc Natl Acad Sci USA* 108: 179 – 184

Okayasu I, Hatakeyama S, Yamada M, Ohkusa T, Inagaki Y, Nakaya R (1990) A novel method in the induction of reliable experimental acute and chronic ulcerative colitis in mice. *Gastroenterology* 98: 694 – 702

Park HS, Goodlad RA, Wright NA (1995) Crypt fission in the small intestine and colon. A mechanism for the emergence of G6PD locus-mutated crypts after treatment with mutagens. *Am J Pathol* 147: 1416 – 1427

Pellegrinet L, Rodilla V, Liu Z, Chen S, Koch U, Espinosa L, Kaestner KH, Kopan R, Lewis J, Radtke F (2011) Dll1- and dll4-mediated notch signaling are required for homeostasis of intestinal stem cells. *Gastroenterology* 140: 1230 – 1240 e1231–1237

Powell AE, Wang Y, Li Y, Poulin EJ, Means AL, Washington MK, Higginbotham JN, Juchheim A, Prasad N, Levy SE, Guo Y, Shyr Y, Aronow BJ, Haigis KM, Franklin JL, Coffey RJ (2012) The pan-ErbB negative regulator Lrig1 is an intestinal stem cell marker that functions as a tumor suppressor. *Cell* 149: 146 – 158

Riccio O, van Gijn ME, Bezdek AC, Pellegrinet L, van Es JH, Zimber-Strobl U, Strobl LJ, Honjo T, Clevers H, Radtke F (2008) Loss of intestinal crypt progenitor cells owing to inactivation of both Notch1 and Notch2 is accompanied by derepression of CDK inhibitors p27Kip1 and p57Kip2. *EMBO Rep* 9: 377 – 383

Sambuy Y, De Angelis I, Ranaldi G, Scarino ML, Stammati A, Zucco F (2005) The Caco-2 cell line as a model of the intestinal barrier: influence of cell and culture-related factors on Caco-2 cell functional characteristics. *Cell Biol Toxicol* 21: 1 – 26

Sangiorgi E, Capecchi MR (2008) Bmi1 is expressed *in vivo* in intestinal stem cells. *Nat Genet* 40: 915 – 920

Sato T, Vries RG, Snippert HJ, van de Wetering M, Barker N, Stange DE, van Es JH, Abo A, Kujala P, Peters PJ, Clevers H (2009) Single Lgr5 stem cells build crypt-villus structures *in vitro* without a mesenchymal niche. *Nature* 459: 262 – 265

Schindelin J, Arganda-Carreras I, Frise E, Kaynig V, Longair M, Pietzsch T, Preibisch S, Rueden C, Saalfeld S, Schmid B, Tinevez JY, White DJ, Hartenstein V, Eliceiri K, Tomancak P, Cardona A (2012) Fiji: an open-source platform for biological-image analysis. *Nat Methods* 9: 676 – 682

Takeda N, Jain R, LeBoeuf MR, Wang Q, Lu MM, Epstein JA (2011) Interconversion between intestinal stem cell populations in distinct niches. *Science* 334: 1420 – 1424

Tetteh PW, Basak O, Farin HF, Wiebrands K, Kretzschmar K, Begthel H, van den Born M, Korving J, de Sauvage F, van Es JH, van Oudenaarden A, Clevers H (2016) Replacement of lost Lgr5-positive stem cells through plasticity of their enterocyte-lineage daughters. *Cell Stem Cell* 18: 203 – 213

Tian H, Biehs B, Warming S, Leong KG, Rangell L, Klein OD, de Sauvage FJ (2011) A reserve stem cell population in small intestine renders Lgr5-positive cells dispensable. *Nature* 478: 255 – 259

Tomic G, Morrissey E, Kozar S, Ben-Moshe S, Hoyle A, Azzarelli R, Kemp R, Chilamakuri CSR, Itzkovitz S, Philpott A, Winton DJ (2018) Phospho-regulation of ATOH1 is required for plasticity of secretory progenitors and tissue regeneration. *Cell Stem Cell* 23: 436 – 443 e437

Yan KS, Chia LA, Li X, Ootani A, Su J, Lee JY, Su N, Luo Y, Heilshorn SC, Amieva MR, Sangiorgi E, Capecchi MR, Kuo CJ (2012) The intestinal stem cell

markers Bmi1 and Lgr5 identify two functionally distinct populations. *Proc Natl Acad Sci USA* 109: 466 – 471

Yan KS, Gevaert O, Zheng GXY, Anchang B, Probert CS, Larkin KA, Davies PS, Cheng ZF, Kaddis JS, Han A, Roelf K, Calderon RI, Cynn E, Hu X, Mandleywala K, Wilhelmy J, Grimes SM, Corney DC, Boutet SC, Terry JM *et al* (2017) Intestinal enteroendocrine lineage cells possess homeostatic and injury-inducible stem cell activity. *Cell Stem Cell* 21: 78 – 90 e76

Yui S, Azzolin L, Maimets M, Pedersen MT, Fordham RP, Hansen SL, Larsen HL, Guiu J, Alves MRP, Rundsten CF, Johansen JV, Li Y, Madsen CD, Nakamura T, Watanabe M, Nielsen OH, Schweiger PJ, Piccolo S, Jensen KB (2018) YAP/TAZ-dependent reprogramming of colonic epithelium links ECM remodeling to tissue regeneration. *Cell Stem Cell* 22: 35 – 49 e37

Zachos NC, Kovbasnjuk O, Foulke-Abel J, In J, Blutt SE, de Jonge HR, Estes MK, Donowitz M (2016) Human enteroids/colonoids and intestinal organoids functionally recapitulate normal intestinal physiology and pathophysiology. *J Biol Chem* 291: 3759 – 3766

